

Electronic Supplementary Information

Green synthesis of cobalt ferrite from rotten passion fruit juice and application as an electrocatalyst for the hydrogen evolution reaction

Rochelin Prosper Medang^a, Roussin Lontio Fomekong^b, Edwin Akongnwi Nforna^c Hypolite Mathias Kamta Tedjieukeng^b, Cédrik Ngnintedem Yonti^b, Patrice Kenfack Tsobnang^{*d}, John Ngolui Lambi^b and Dieudonné Bitondo^{a,e}

^aLaboratoire de recherche Energie, Matériaux, Modélisation et Méthode (E3M), École Nationale Supérieure Polytechnique de Douala, Université de Douala, Douala, Cameroun

^bDepartment of Chemistry, Higher Teacher Training College, University of Yaounde I

^cDepartment of Fundamental Sciences, Higher Technical Teacher Training College, University of Bamenda

^dDepartment of Chemistry, University of Dschang, P.O. Box 67, Dschang, Cameroon

^eDépartement Qualité Industrielle, Hygiène, Sécurité Industrielle et Génie de l'Environnement, École Nationale Supérieure Polytechnique de Douala, Université de Douala, Douala, Cameroun

*Corresponding authors. E-mail addresses: Patrice.kenfack@univ-dschang.org, pakenfack@mail.com (P.Kenfack Tsobnang)

Table S1. Titration of the passion fruit juice

	1	2	3	Average
V_{fruit}(mL)	10,00 ± 0,01	10,00 ± 0,01	10,00 ± 0,01	10,00 ± 0,01
V_{NaOH}(mL)	45,00 ± 0,01	44,00 ± 0,01	46,00 ± 0,01	45,00 ± 0,01

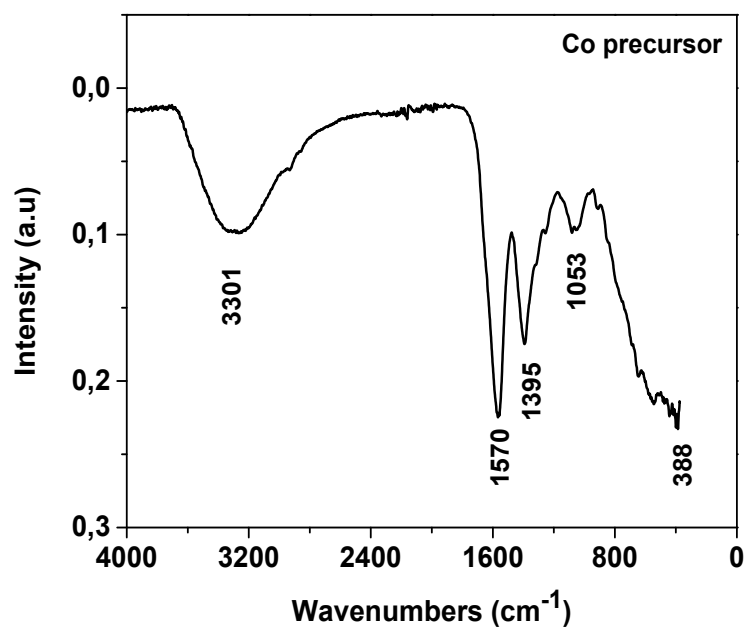


Figure S1. FTIR of Co precursor

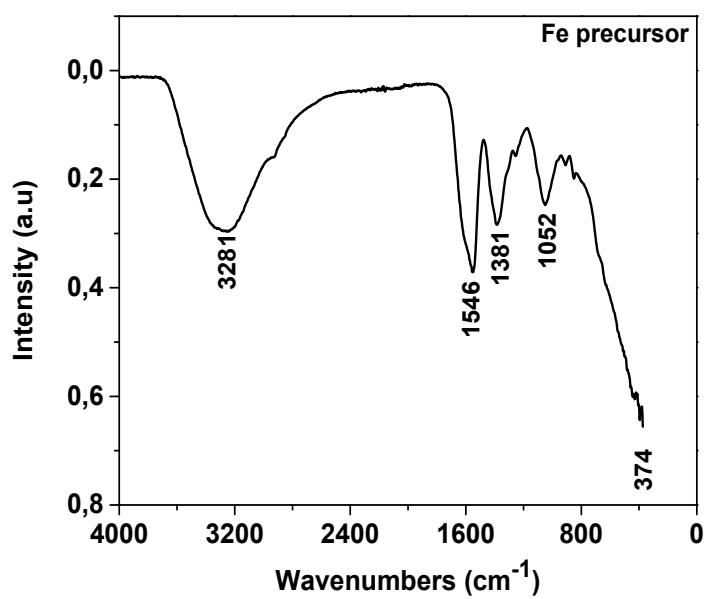


Figure S2. FTIR of Fe precursor

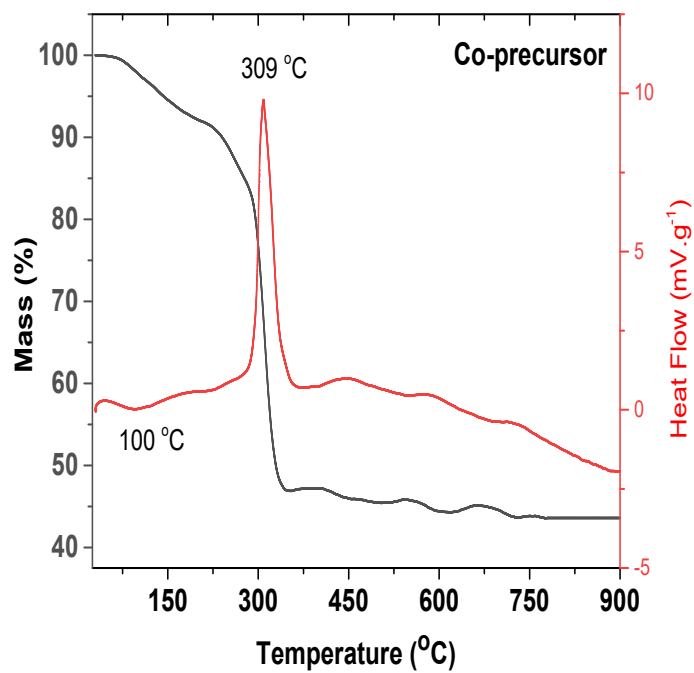


Figure S3. Thermogravimetric analysis of Co precursor

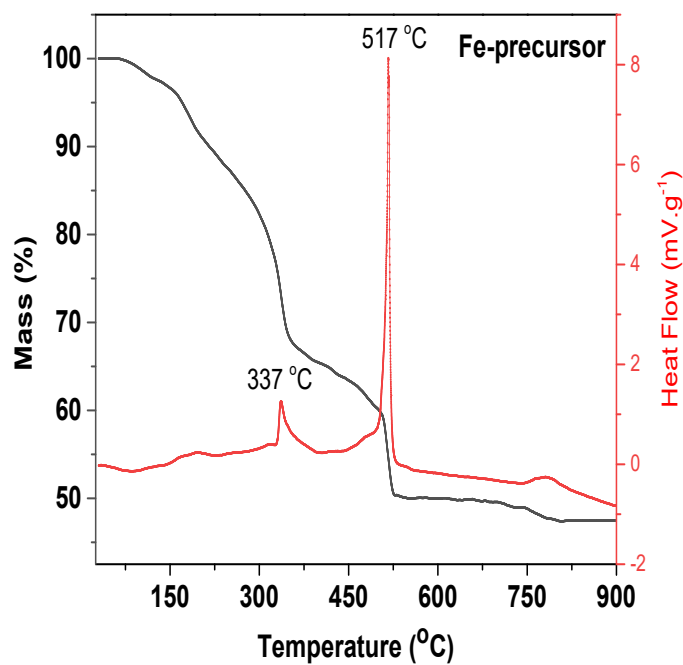


Figure S4. Thermogravimetric analysis of Fe precursor

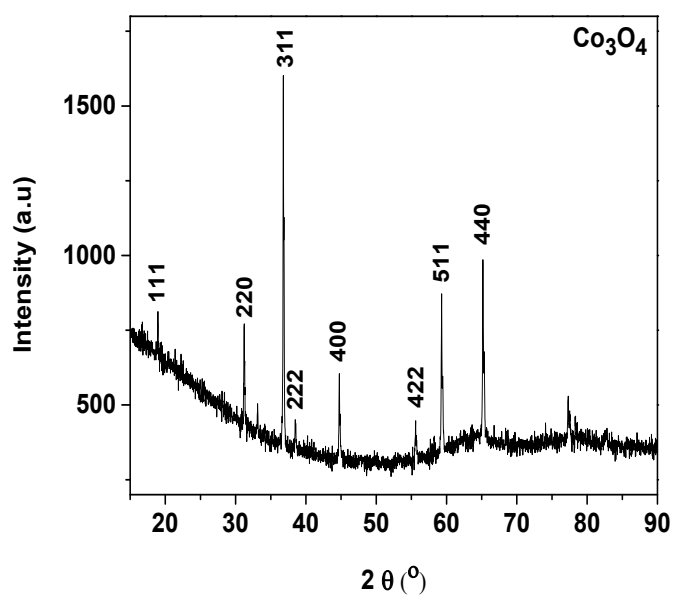


Figure S5. X-ray powder diffraction pattern of the residue from the thermal decomposition of the Co precursor

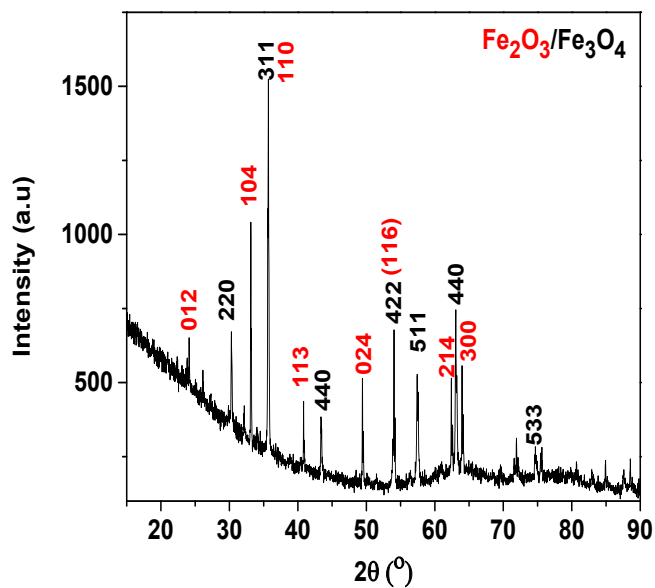


Figure S6. X-ray powder diffraction pattern of the residue from the thermal decomposition of the Fe precursor

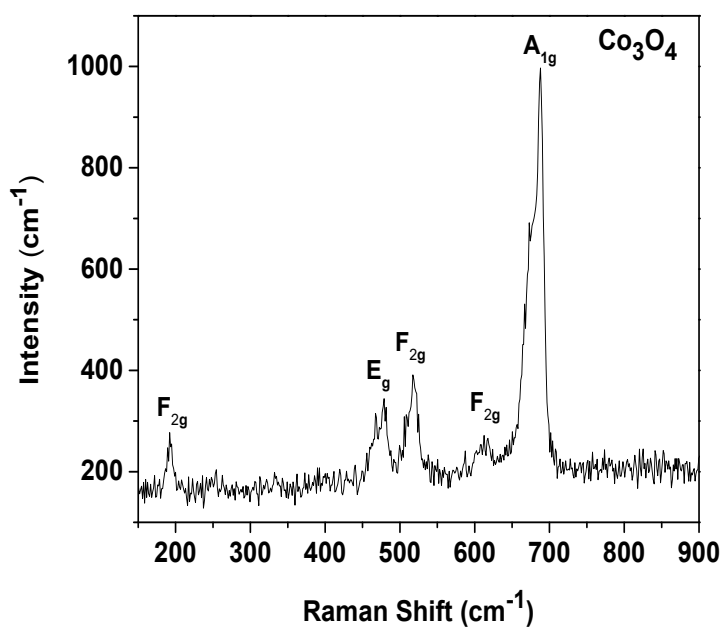


Figure S7. Experimental Raman analysis of the residue from the thermal decomposition of the Co precursor

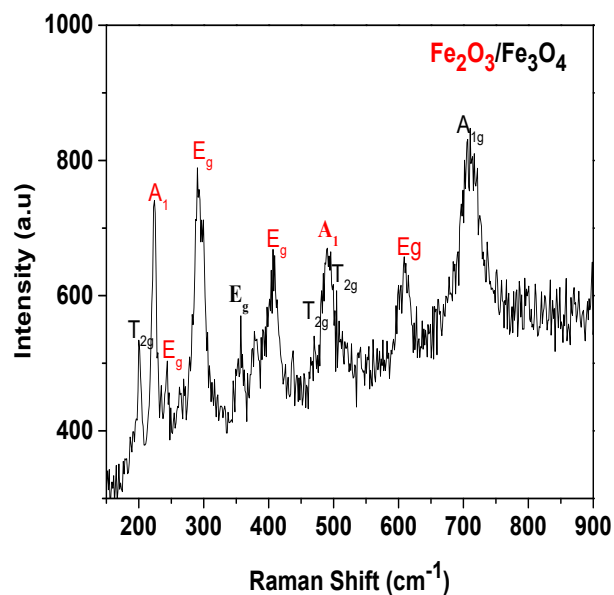


Figure S8. Experimental Raman analysis of the residue from the thermal decomposition of the Fe precursor

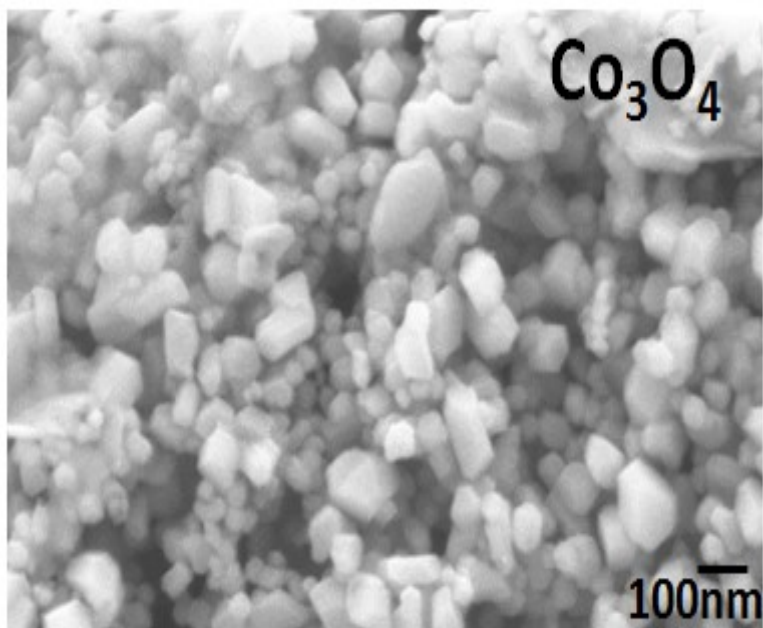


Figure S9. SEM image of the Co_3O_4 on a reduced scale $\sim 100\text{nm}$

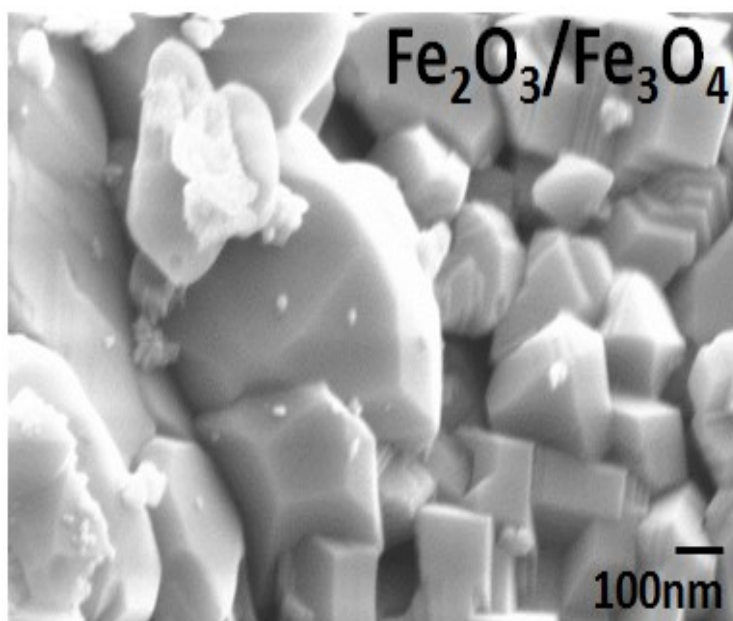


Figure S10. SEM image of the $\text{Fe}_2\text{O}_3/\text{Fe}_3\text{O}_4$ on a reduced scale $\sim 100\text{nm}$

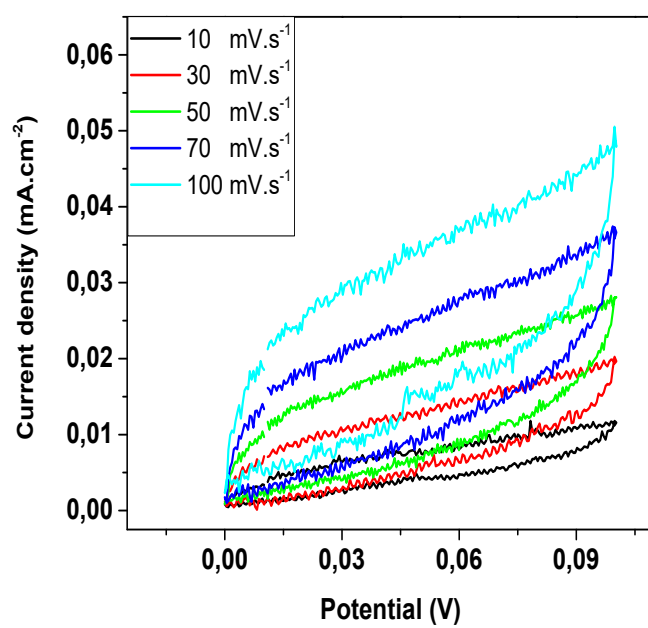


Figure S11. Cyclic voltametric curves of CoFe₂O₄ at different scanning speeds